USCAP

ARTICLE

Check for updates

# Epstein–Barr-virus-positive large B-cell lymphoma associated with breast implants: an analysis of eight patients suggesting a possible pathogenetic relationship

L. Jeffrey Medeiros[1], Mario L. Marques-Piubelli[2], Valentina F. I. Sangiorgio[3], Roberto Ruiz-Cordero[4], Francisco Vega[1], Andrew L. Feldman[5], Jennifer R. Chapman[6], Mark W. Clemens[7], Kelly K. Hunt[8], Mark G. Evans[1], Christine Khoo[9], Stephen Lade[9], Mark Silberman[10], Jerzy Morkowski[11], Edward M. Pina[12], Daniel C. Mills[13], Christopher M. Bates[14], Winston B. Magno[15], Aliyah R. Sohani[16], Beth A. Sieling[17], Joseph M. O'Donoghue[18], Chris M. Bacon[19], Neill Patani[20], Despina Televantou[21], Suzanne D. Turner[22], Laura Johnson[23], Fiona MacNeill[24], Andrew C. Wotherspoon[25], Swaminathan P. Iyer[26], Luis E. Malpica[26], Keyur P. Patel[1], Jie Xu[1] and Roberto N. Miranda[1]✉



Breast implant anaplastic large cell lymphoma (ALCL) is a T-cell neoplasm arising around textured breast implants that was recognized recently as a distinct entity by the World Health Organization. Rarely, other types of lymphoma have been reported in patients with breast implants, raising the possibility of a pathogenetic relationship between breast implants and other types of lymphoma. We report eight cases of Epstein–Barr virus (EBV)-positive large B-cell lymphoma associated with breast implants. One of these cases was invasive, and the other seven neoplasms were noninvasive and showed morphologic overlap with breast implant ALCL. All eight cases expressed B-cell markers, had a non-germinal center B-cell immunophenotype, and were EBV+ with a latency type III pattern of infection. We compared the noninvasive EBV+ large B-cell lymphoma cases with a cohort of breast implant ALCL cases matched for clinical and pathologic stage. The EBV+ large B-cell lymphoma cases more frequently showed a thicker capsule, and more often were associated with calcification and prominent lymphoid aggregates outside of the capsule. The EBV+ B-cell lymphoma cells were more often arranged within necrotic fibrinoid material in a layered pattern. We believe that this case series highlights many morphologic similarities between EBV+ large B-cell lymphoma and breast implant ALCL. The data presented suggest a pathogenetic role for breast implants (as well as EBV) in the pathogenesis of EBV+ large B-cell lymphoma. We also provide some histologic findings useful for distinguishing EBV+ large B-cell lymphoma from breast implant ALCL in this clinical setting.

*Modern Pathology* (2021) 34:2154–2167; https://doi.org/10.1038/s41379-021-00863-1

## INTRODUCTION

Non-Hodgkin lymphomas arising in the breast are rare and account for ~0.5% of all breast tumors and for 2.2% of all extranodal lymphomas [1]. About 90% of lymphomas arising in the breast are of B-cell lineage and the most common types are extranodal marginal zone lymphoma and diffuse large B-cell lymphoma [1]. About 10% of breast lymphomas are of T-cell lineage, and the breast is also commonly involved by various types of systemic lymphoma.

Breast implant anaplastic large cell lymphoma (ALCL) is a relatively recently recognized type of T-cell lymphoma. The first case of breast implant ALCL arising in proximity to a saline-filled breast implant was reported by Keech and Creech in 1997 [2],

[1]Department of Hematopathology, The University of Texas MD Anderson Cancer Center, Houston, TX, USA. [2]Department of Translational Molecular Pathology, The University of Texas MD Anderson Cancer Center, Houston, TX, USA. [3]Division of Hematopathology, Department of Cellular Pathology, The Royal London Hospital. Barts Health NSH Trust, London, UK. [4]Department of Pathology, University of California San Francisco, San Francisco, CA, USA. [5]Division of Hematopathology, Mayo Clinic College of Medicine, Rochester, MN, USA. [6]Department of Pathology and Laboratory Medicine, University of Miami/Jackson Memorial Hospital, Miami, FL, USA. [7]Department of Plastic Surgery, The University of Texas MD Anderson Cancer Center, Houston, TX, USA. [8]Department of Breast Surgical Oncology, The University of Texas MD Anderson Cancer Center, Houston, TX, USA. [9]Pathology Department, Peter MacCallum Cancer Centre, Melbourne, VIC, Australia. [10]Clinical Pathology Laboratory, Austin, TX, USA. [11]MLD Pathology, Houston, TX, USA. [12]Pina Cosmetic Surgery, Dpt Surgery HCA Houston Healthcare Southeast, Houston, TX, USA. [13]Aesthetic Plastic Surgical Institute, Laguna Beach, CA, USA. [14]Ponte Vedra Plastic Surgery, Ponte Vedra Beach, FL, USA. [15]Regional Healthcare Associates, LLC, Waterbury, CT, USA. [16]Department of Pathology, Massachusetts General Hospital, Harvard Medical School, Boston, MA, USA. [17]Department of Surgery, St. Mary's Hospital, Trinity Health of New England, Waterbury, CT, USA. [18]Department of Plastic Surgery, Newcastle Upon Tyne Hospitals NHS Foundation Trust, Newcastle Upon Tyne, UK. [19]Department of Cellular Pathology, Newcastle Upon Tyne Hospitals NHS Foundation Trust and Translational and Clinical Research Institute, Newcastle University, Newcastle Upon Tyne, UK. [20]Department of Breast Surgery, University College London Hospitals NHS Foundation Trust, London, UK. [21]Department of Cellular Pathology, Newcastle Upon Tyne Hospitals NHS Foundation Trust, Newcastle Upon Tyne, UK. [22]Division of Cellular and Molecular Pathology, Department of Pathology, University of Cambridge, Cambridge, UK. [23]Department of Surgery, Barts Health NHS Trust, London, UK. [24]Department of Surgery, The Royal Marsden NHS Foundation Trust, London, UK. [25]Department of Histopathology, The Royal Marsden NHS Foundation Trust, London, UK. [26]Department of Myeloma and Lymphoma, The University of Texas MD Anderson Cancer Center, Houston, TX, USA. ✉email: roberto.miranda@mdanderson.org

Received: 8 March 2021 Revised: 17 June 2021 Accepted: 18 June 2021
Published online: 5 July 2021

although it is likely that cases occurred earlier but were designated using different diagnostic terms [3]. Since then, the association of breast implants with ALCL has become established, and breast implant ALCL was recently accepted as a distinct entity by the World Health Organization (WHO) [4, 5]. Breast implant ALCL arises around breast implants, almost exclusively in association with textured implants, and is usually confined by a fibrous capsule. The lymphoma cells uniformly and strongly express CD30 as well as T-cell antigens, carry monoclonal T-cell receptor gene rearrangements, and lack *ALK* rearrangement or expression. Breast implant ALCL is usually detected at an early stage, and most patients can be cured by removal of the implants and complete excision of the capsule [6–8]. A small subset of patients requires adjuvant/neo-adjuvant systemic therapy, particularly those patients with tumors that invade beyond the capsule, including patients with disease invading into the chest wall and thoracic structures, regional lymph nodes, or rare patients who develop distant metastases [6, 9].

In recent years, anecdotal reports of B-cell and "non-ALCL" T-cell lymphomas have been reported in patients with breast implants [10–17]. In the past year, two reports described a total of six cases of EBV+ large B-cell lymphoma associated with breast implants [18, 19]. The pathogenesis and optimal classification using the WHO classification for these neoplasms is unclear.

In this study, we describe the clinicopathologic features of eight cases of EBV+ large B-cell lymphoma arising in patients with breast implants, including seven noninvasive cases and one invasive neoplasm. We discuss the pathologic and immunophenotypic features of these neoplasms and compare the noninvasive neoplasms with a matched group of breast implant ALCL cases. We also make some suggestions regarding the possible pathogenesis and classification of EBV+ large B-cell lymphoma arising in patients with breast implants.

## MATERIALS AND METHODS

### Clinical data

We searched the files of the Department of Hematopathology at The University of Texas MD Anderson Cancer Center, as well as the files of collaborative institutions for patients who had breast implants and developed EBV+ large B-cell lymphoma. To be included in this study, we required that pathologic specimens be available for review, including the results of immunohistochemical and in situ hybridization studies. The clinical features of these patients were obtained by review of the medical records. Clinical data collected included age, gender, reason for implant, type and surface (textured or smooth) of implants, implant manufacturer, time from implant insertion to diagnosis, clinical manifestations at presentation, clinical diagnosis after surgery, surgical procedures at and after diagnosis, treatment or adjuvant radiation or chemotherapy, clinical follow up, and final outcome. Time from implantation to lymphoma diagnosis was defined as the interval between the first breast implant surgery and the time lymphoma was diagnosed, regardless of whether a patient had intervening surgical procedures. The Institutional Review Board at MD Anderson approved this study.

### Histology and immunohistochemistry

Each case of EBV+ large B-cell lymphoma in this study was composed of large cells positive for B-cell markers, such as CD20, CD79a, or PAX5, and EBV-encoded small RNA (EBER), as defined by others previously [18, 19].

Hematoxylin and eosin-stained tissue sections prepared from formalin-fixed, paraffin-embedded tissue blocks were reviewed. Immunohistochemical studies were performed at referral laboratories or our institution. For cases in our laboratory, 4-µm-thick sections were processed on a Leica immunostainer (Leica Biosystems Inc., Buffalo Grove, IL, USA), following the manufacturer's instructions. The following antibodies were used: CD3 (OKT3) and granzyme B (Thermo Fisher Scientific, Waltham, MA, USA); CD4 (SP35) Cell Marque, Rocklin, CA, USA); CD5 (SP4) and CD8 (C8/144B) (LabVision, Fremont, CA, USA); CD10 (56C6), CD138 (SOC32) and HHV-8 (Novocastra/Leica Biosystems Inc); EB nuclear antigen 2 (R3) (Sigma-Aldrich, St Louis, MO, USA); MYC (Ventana, Oro Valley, AZ, USA), PAX5 (clone 24; BD Biosciences, Franklin Lakes, NJ, USA); TIA-1 (Immunotech, Swanton, VT, USA); CD15 (Carb-3), CD20 (L26), CD30 (Ber-H2), CD43 (DF-T1), CD45 (2B11 + PD7/26), CD79a (JCB117), anaplastic lymphoma kinase 1, Bcl-6, epithelial membrane antigen (E29), EBV latent membrane protein-1 (LMP-1), Ki-67 (MIB-1) and MUM-1/IRF4 (Dako, Carpinteria, CA, USA). Diaminobenzidine was used as the chromogen, and hematoxylin was used as counterstain.

### In situ hybridization

In situ hybridization analysis for EBER was performed using a fluorescein-labeled peptide nucleic acid probe (Dako) in conjunction with the Dako peptide nucleic acid ISH detection kit for formalin-fixed, paraffin-embedded tissue sections.

### Polymerase chain reaction

Polymerase chain reaction (PCR)-based methods were used to assess the configuration of *IGH*, *TRB*, and *TRG* [20]. For this purpose, DNA was extracted from fixed, paraffin-embedded tissue sections of tumor blocks using standard methods.

### Comparison with breast implant ALCL

For comparison, we identified 14 previously reported patients with noninvasive breast implant ALCL stage matched with the 7 noninvasive cases of EBV+ LBCL. We also compared five patients with invasive breast implant ALCL [6, 7, 21, 22], to contrast with the invasive cases as noted in Tables 4 and 5. Cases of breast implant ALCL were classified according to current WHO classification criteria [4, 5]. Six cases of breast implant ALCL were shown to carry monoclonal *TRB* and *TRG* rearrangements.

In these comparisons, we assessed the following histologic features: capsule thickness, presence of a synovium-like lining layer, or granular necrosis on the luminal side of the capsule; distribution and characteristics of the lymphoma cells, and presence versus absence of the following features: hallmark cells (kidney/horseshoe shape), plasma cells, eosinophils, foamy histiocytes, calcification, refringent material consistent with silicone material and lymphoid aggregates on the outer aspect of the capsule.

### Statistical analysis

The unpaired *t*-test, Chi-square, and Fisher's exact test were performed using GraphPad Prism version 8.0.0 for Windows (GraphPad Software, San Diego, CA, USA) www.graphpad.com. A $P$ value $< 0.05$ was considered significant.

## RESULTS

### Clinical features of patients with EBV+ large B-cell lymphoma

The study cohort included eight women diagnosed with EBV+ large B-cell lymphoma; seven cases were noninvasive (Table 1) and one patient presented with an invasive mass. Two noninvasive cases were published previously [19, 23]. In the noninvasive group, the median age at diagnosis was 65 years (range, 47–71 years). Six (86%) patients presented with capsular induration considered clinically to be contracture (Fig. 1A). On imaging studies, capsular thickening with minimal or no fluid was noted (Fig. 1B). The reasons for implant were known in six patients: four (67%) underwent bilateral breast implant surgery for cosmetic reasons and two (33%) underwent reconstruction after breast cancer. All patients were apparently immunocompetent and seronegative for human immunodeficiency virus. All patients had a history of exposure to textured breast implants. The filling of the implants was known for five patients: silicone in four (80%) and saline in one (20%). The manufacturers of the implants were available in seven patients; Allergan, Inc. (Dublin, Ireland) in six patients and Silimed, Inc. (Rio de Janeiro, Brazil) in one patient. The median interval from implant placement to development of lymphoma was 10 years (range, 4–26 years). Six patients developed discomfort around an implant. One patient was asymptomatic; in this case, the neoplasm was discovered by imaging studies performed to assess for heart disease. All patients presented with clinical Ann Arbor stage IE disease.

The patient who had an invasive EBV+ large B-cell lymphoma was 48 years old. She was referred with recent nodularity

**Table 1.** Clinical features of patients with noninvasive BI EBV+ LBCL and breast implant ALCL (pT2).

| Features | BI EBV+ LBCL, $n = 7$ | Breast implant ALCL, $n = 14$ | $p$ value |
|---|---|---|---|
| Age at diagnosis, median (years, range) | 65 (47–71) | 54.5 (40–77) | 0.699 |
| Reason for implant | $n = 6$ | $n = 14$ | 0.6285 |
| Cosmetic; $n$ (%) | 4 (66%) | 6 (43%) | |
| Reconstruction for breast cancer; $n$ (%) | 2 (33%) | 8 (57%) | |
| Implant features | | | |
| Surface | $n = 7$ | $n = 10$ | >0.999 |
| Textured; $n$ (%) | 7 (100%) | 10 (100%) | |
| Filling | $n = 5$ | $n = 13$ | >0.999 |
| Silicone; $n$ (%) | 4 (80%) | 9 (69%) | |
| Saline; $n$ (%) | 1 (20%) | 4 (31%) | |
| Manufacturer | $n = 7$ | $n = 11$ | 0.3294 |
| Allergan; $n$ (%) | 6 (85%) | 10 (91%) | |
| Silimed; $n$ (%) | 1 (15%) | 0 (0%) | |
| Eurosilicon | 0 (0%) | 1 (9%) | |
| Time from implantation to lymphoma, median (years, range) | 10 (4–26) | 11 (4–34) | 0.8443 |
| Clinical manifestation | $n = 7$ | $n = 12$ | |
| Swelling | 0 (0%) | **11 (92%)** | **0.0002** |
| Discomfort | 6 (86%) | 0 (0%) | |
| Asymptomatic | 1 (14%) | 1 (8%) | |
| Clinical diagnosis at presentation | $n = 7$ | $n = 14$ | |
| Capsular contracture; $n$ (%) | **6 (86%)** | 2 (14%) | **0.0025** |
| Effusion/"seroma"; $n$ (%) | 0 (0%) | **11 (79%)** | **0.0025** |
| Incidental | 1 (14%) | 1 (7%) | |
| Clinical staging | $n = 7$ | $n = 14$ | >0.999 |
| IE; $n$ (%) | 7 (100%) | 14 (100%) | |
| Pathological staging | $n = 7$ | $n = 14$ | >0.999 |
| pT2 | 7 (100%) | 14 (100%) | |
| Management and therapy | $n = 7$ | $n = 14$ | |
| Complete capsulectomy and implant removal; $n$ (%) | 7 (100%) | 14 (100%) | |
| Adjuvant chemotherapy; $n$ (%) | 1[a] (14%) | 5 (35%) | |
| Outcome | | | |
| Follow up median (months, range) | 8 (1–96) | 63 (1–96) | >0.999 |
| Alive with no evidence of disease; $n$ (%) | 7 (100%) | 12 (86%) | |
| Dead of other causes, $n$ (%) | 0 (0%) | 2 (14%) | |

BI EBV+ LBCL: breast implant-associated EBV+ large B-cell lymphoma, ALCL: anaplastic large cell lymphoma, pT2: pathologic stage 2 means lymphoma cells confined to luminal side of capsule; minimal interaction with inflammatory cells. Bold $p$ value indicates that the comparison is statistically significant. Bold result and percentage indicate that the value is statistically significant.

[a]Three cycles of rituximab, cyclophosphamide, adriamycin, vincristine, prednisone, and intrathecal methotrexate.

alongside longstanding breast implants. Biopsies of the implant capsules and adjacent breast parenchyma were performed, and the specimens were reported to show reactive changes. One year later, the patient underwent replacement of the implants, and 1 year thereafter she presented with a left axillary mass.

### Therapy and follow-up

All patients underwent complete capsulectomy with implant removal. One of seven patients with noninvasive EBV+ large B-cell lymphoma received three cycles of adjuvant chemotherapy with rituximab, cyclophosphamide, doxorubicin, vincristine, and prednisone (R-CHOP), as well as intrathecal methotrexate. The median follow-up interval was 8 months (range, 1–96 months), and at last follow up all patients were alive with no evidence of disease.

The patient who presented with an invasive neoplasm underwent complete capsulectomy, albeit delayed, and axillary lymph node dissection. The patient initially received four cycles of R-CHOP, but developed relapse in the ipsilateral axilla 24 months after chemotherapy. She then received radiation therapy and two cycles of bleomycin, etoposide, adriamycin, cyclophosphamide, vincristine, procarbazine, and prednisone achieving complete remission. The patient subsequently had a second lymphoma relapse presenting as a chest wall mass 21 months after chemotherapy, for which she received ifosfamide, carboplatin, and etoposide. The patient achieved complete remission and received an autologous stem cell transplant (ASCT). She is currently in complete remission 8 months after ASCT and 71 months from the initial diagnosis.

### Macroscopic pathologic features

Gross examination showed rigid and thickened capsules, but no distinct lesions. One noninvasive case resected en bloc revealed a smooth and congested outer surface. Opening this specimen revealed a thick capsule with adherent yellow, viscous material and a small amount of liquefied material over a textured implant (Fig. 1C). The luminal side exhibited partial granularity, but no distinct lesions. In one of these cases, the fibrous lining of the lumen showed focal granularity (Fig. 1D).

### Histologic features

The histologic features of the seven patients with noninvasive EBV+ large B-cell lymphoma are summarized in Table 2. The capsules had a median thickness of 2481 µm (range, 1376–5700) (Fig. 2A–D), with an overall hypocellular appearance. The luminal surface was always covered by granular or necrotic material, but no detached lymphoma cells were noted. No synovium-like cell layer lining the luminal surface was noted. Most of the capsular thickness from the luminal surface to the depths of the capsule appeared eosinophilic. These eosinophilic areas were composed of necrotic ghosts of cells with granular cytoplasm or loose granular material. Focal hematoxyphilic areas corresponding to small clusters of neoplastic cells appeared as layers, sandwiched between layers of granular necrosis (Fig. 2E). The neoplastic cells were large and poorly cohesive, with a moderate amount of cytoplasm, often clear, and a central vesicular nucleus with distinct nucleoli; a number of these cells had undergone necrosis or karyorrhexis (Fig. 2F). No hallmark cells were present. The deeper portions of the capsule showed either necrosis or sclerotic tissue. Focal calcification was present in four of seven (58%) cases. No inflammatory cells were apparently admixed with the lymphoma cells. The deepest portions of the capsule had large lymphoplasmacytic aggregates; occasionally with reactive germinal centers, but no increase of eosinophils.

The patient with invasive EBV+ large B-cell lymphoma had three surgical specimens over time. In the initial specimen, the capsule grossly had an ill-defined area of induration and necrosis adjacent to the implant. Microscopic examination of the partially excised capsule showed a distorted and sclerotic capsule with surrounding breast parenchyma and adipose tissue involved by extensive chronic inflammation. Subtle clusters or individual large cells with pleomorphic nuclei and moderately abundant cytoplasm were immersed in areas of sclerosis, both within the capsule as well as surrounding nearby breast ducts (Fig. 3A). A subset of the large cells had Hodgkin/Reed–Sternberg-like features (Fig. 3B) and involved ~10% of the specimen. In retrospect and further testing, the large cells were positive for PAX5, EBV LMP-1, CD30 (Fig. 3C), CD15, CD45, and MUM-1/IRF4. EBNA-2 was negative. This specimen was misdiagnosed as reactive and definitive therapy was not attempted at the time of initial evaluation.

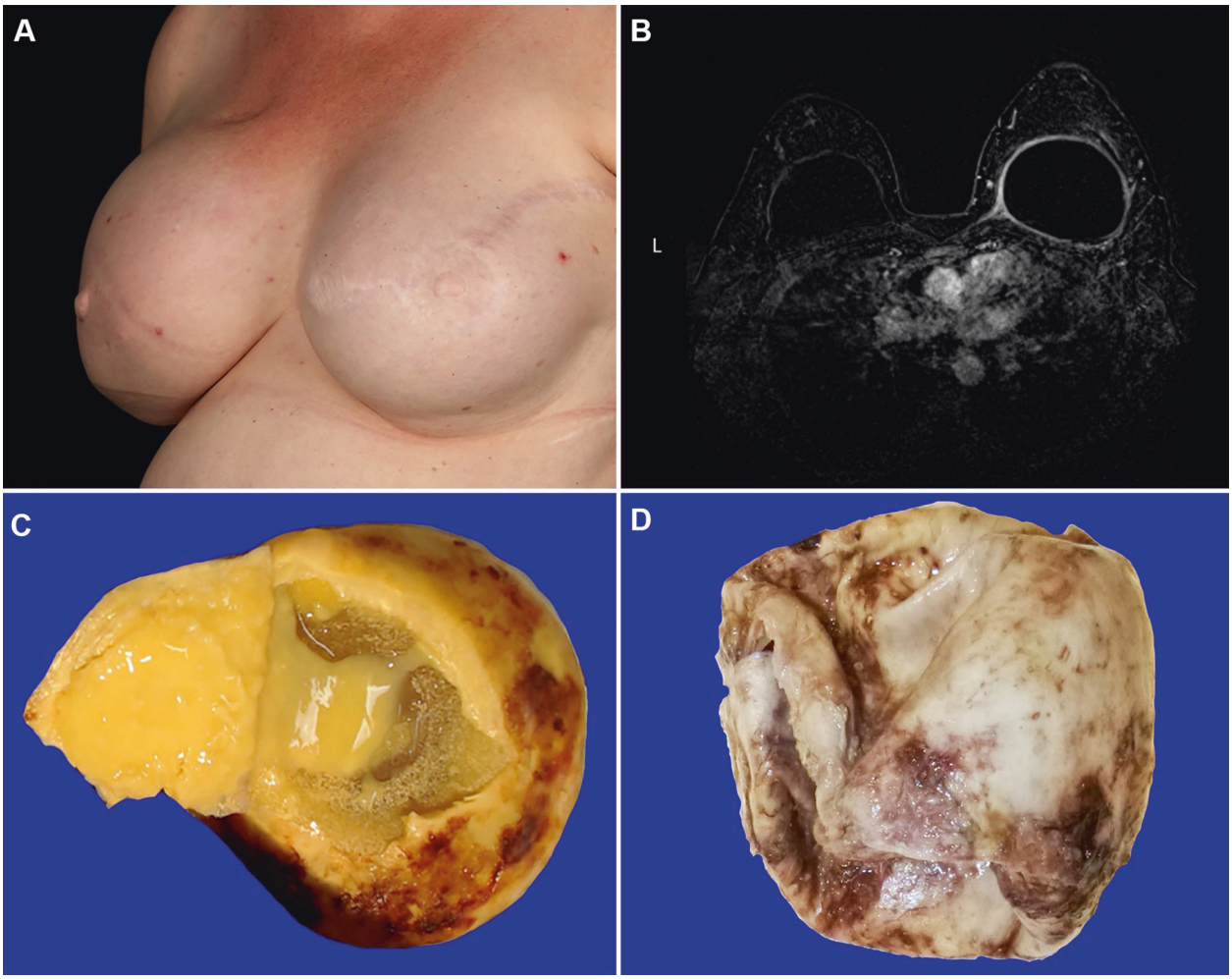


**Fig. 1 Breast-implant-associated Epstein–Barr virus+ (EBV+) large B-cell lymphoma: clinical, imaging, and macroscopic features.** **A** Clinical image depicts increased projection and elevation of the right breast implant, consistent with contracture, in a patient with previous reconstructive surgery following breast cancer. **B** Magnetic resonance imaging of chest, from a different patient who received cosmetic augmentation implants, and manifested with recent onset of local pain. The image shows a thickened peri-implant capsule of the right side; note the lack of effusion, characteristic of this entity. **C** Gross appearance of fresh, unfixed, en bloc resection of capsule containing the implant. The outer surface is smooth. The specimen is partially opened and displays a rigid and thickened capsule, as well as a minimal amount of liquified material, under which a textured implant is present. **D** Formalin-fixed complete capsulectomy of another case of breast implant EBV+ large B-cell lymphoma displays a tan-colored, rough surface with focal areas of granularity.

**Table 2.** Pathologic features of patients with noninvasive BI EBV+ LBCL and breast implant ALCL (pT2).

| Features | BI EBV+ LBCL, $n = 7$ | Breast implant ALCL, $n = 14$ | $p$ value |
|---|---|---|---|
| Capsular thickness | | | |
| Median (μm, range) | **2481 (1376–5700)** | 1120 (543–4347) | **0.0439** |
| Synovium-like lining | 0/7 (0%) | 3/14 (21%) | 0.1859 |
| Granular necrosis in lumen | 7/7 (100%) | 14/14 (100%) | >0.999 |
| Layering of lymphoma cells | **6/7 (86%)** | 3/14 (21%) | **0.005** |
| Hallmark cells | 0/7 (0%) | **10/14 (70%)** | **0.0039** |
| Plasma cells | 6/7 (86%) | 9/14 (64%) | 0.3055 |
| Eosinophils | 0/7 (0%) | 4/14 (30%) | 0.255 |
| Outer capsule lymphoid aggregates | **7/7 (100%)** | 0/14 (0%) | **0.0001** |
| Foamy histiocytes | **2/7 (29%)** | 0/14 (0%) | **0.0355** |
| Silicone fragments | 4/7 (58%) | 11/14 (79%) | 0.3055 |
| Calcification in lumen | **4/7 (58%)** | 1/14 (7%) | **0.0112** |

Bold $p$ value indicates that comparison is statistically significant. Bold ratio and percentage indicate the value which is statistically significant.

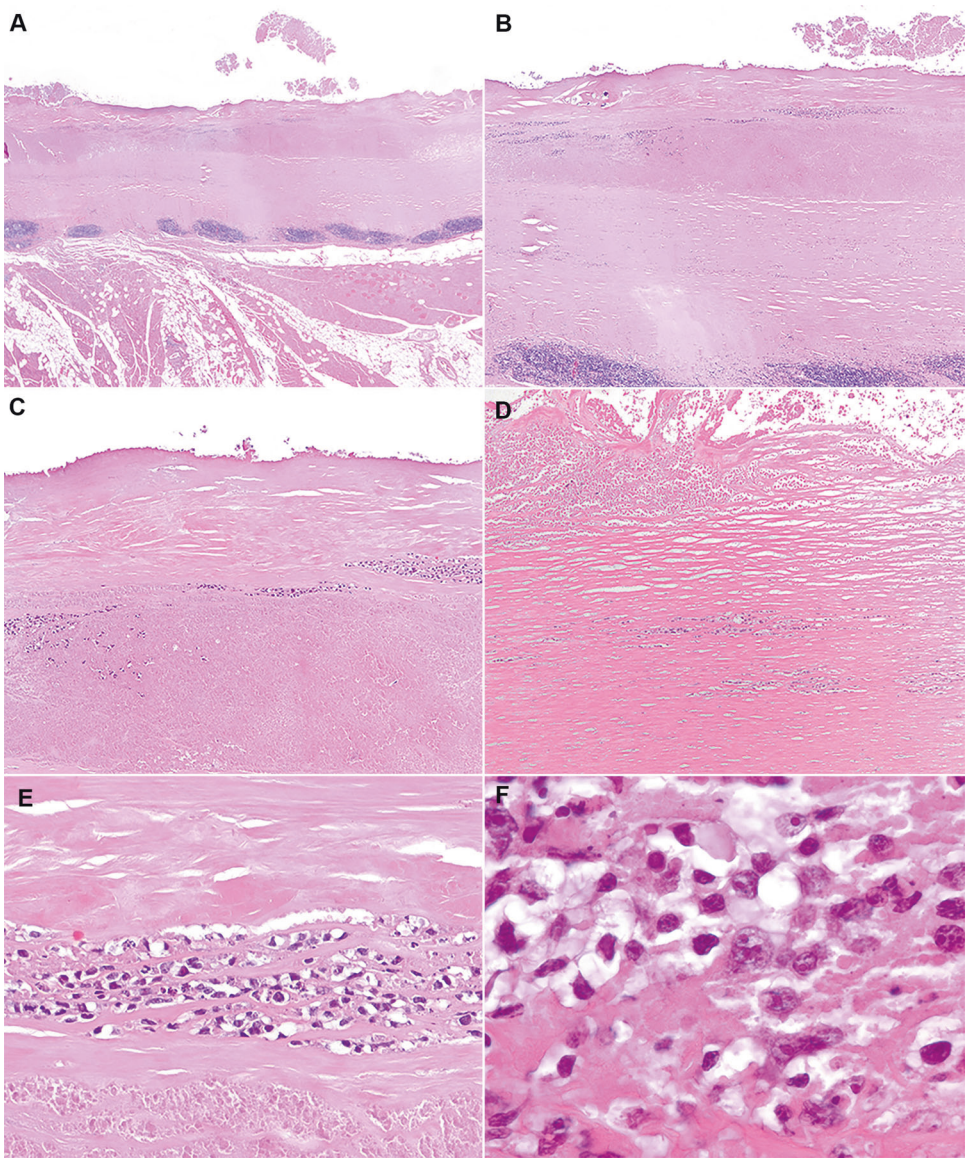


**Fig. 2 Noninvasive breast implant EBV+ large B-cell lymphoma: histopathologic features. A** Cross section of capsule with the luminal side on top and skeletal muscle on the bottom. The luminal side displays granular material which is attached (left) or detached (middle). The capsule is thickened and eosinophilic, while the outer aspect of the capsule displays multiple lymphoid aggregates. The bottom of the figure shows skeletal muscle and adipose tissue that surrounds the capsule. The presence of skeletal muscle indicates that if removed intact, this was an en bloc resection. Hematoxylin and eosin, 10×. **B** This cross section shows the luminal side on top, where granular necrosis is noted; most of the luminal surface is fibrotic and has focal calcification (left). The next level shows layered clusters of cells, followed by extensive areas of necrosis that appears as eosinophilic granular material, and deeper to this, there is thick collagen fibrosis. The outer most level of the capsule shows aggregates of lymphocytes. Hematoxylin and eosin, 40×. **C** Detail of the luminal side of the capsule shows an acellular surface with streaks of necrosis, followed by pink fibrosis and layered clusters of cells, and massive necrosis on the bottom of the image. Hematoxylin and eosin, 100×. **D** Section of capsule of another case shows the luminal side on the top, where there are abundant ghost cells amidst sclerosis. The middle shows scattered lymphoma cells, which are focally in clusters. Hematoxylin and eosin, 100×. **E** Cluster of lymphoma cells surrounded by sclerosis on top and necrosis at the bottom. The lymphoma cells are uniform, intermediate to large in size, with oval to irregular nuclear contours, vesicular chromatin, and moderately abundant clear cytoplasm. This field shows viable lymphoma cells, although there are several cells undergoing karyorrhexis and necrosis. Hematoxylin and eosin, 400×. **F** Lymphoma cells show vesicular chromatin with 1–3 small nucleoli, and moderately abundant clear cytoplasm. The small karyorrhectic, and ghost cells are lymphoma cells captured at different stages of necrosis. Hematoxylin and eosin, 1000×.

An excision was performed 2 months later for complete removal of the lesion. In retrospect, the surgical margins were involved by lymphoma cells. The implant was removed and replaced 1 year later; no systemic therapy was administered. Twenty-four months following initial presentation, the patient developed a left axillary mass involved microscopically by diffuse large B-cell lymphoma (Fig. 3D). Foci of necrosis with numerous neutrophils and occasional eosinophils were present. The immunophenotype and EBV reactivity were similar in the original lesion as well as in the lymph node. Additional surgery was performed to obtain clear surgical margins.

### Immunohistochemical and molecular features

The immunohistochemical features of the EBV+ large B-cell lymphoma cases are summarized in Tables 3 and 5 (Fig. 4). The

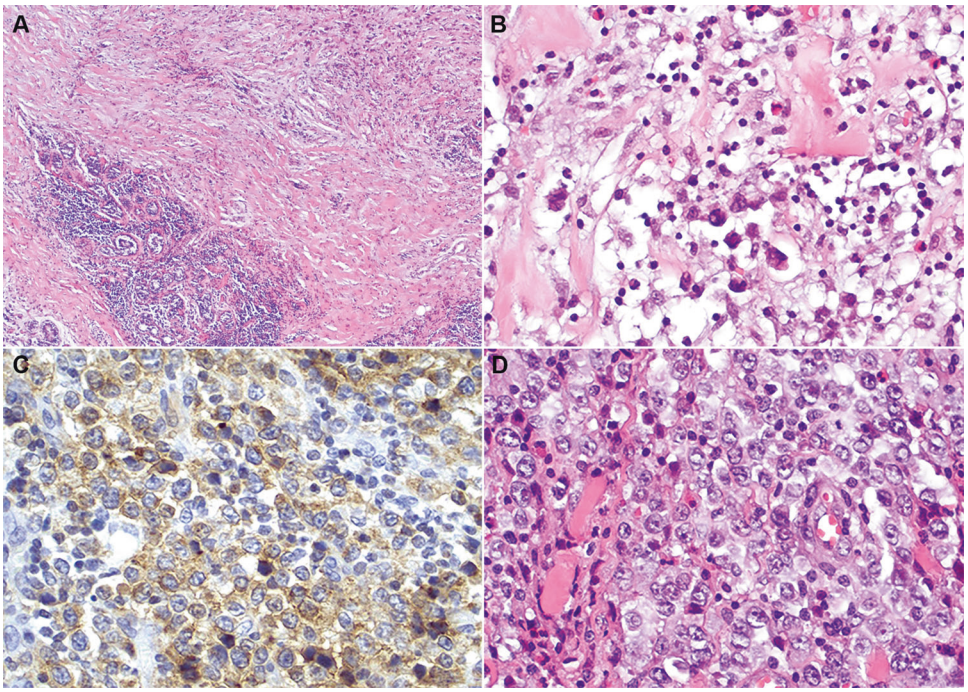


**Fig. 3 EBV+ large B-cell lymphoma, not otherwise specified, arising in a patient with breast implants. A** Lymphohistiocytic infiltrate around a breast implant that the patient referred to as a nodule. The infiltrate involves fibrous capsule (top right) that displays sclerosis and inflammatory cells. The infiltrate permeates into surrounding breast ducts (bottom left). Hematoxylin and eosin, 200×. **B** Detail of the infiltrate as noted at initial presentation. The infiltrate in both the capsule as well as around breast ducts was similar and was composed of occasional large hyperchromatic cells with lobated nuclei and distinct nucleoli admixed with numerous small lymphocytes, histiocytes, and scattered eosinophils with a highly sclerotic background. This infiltrate was initially misinterpreted as reactive. **C** Immunohistochemistry of the tumor mass demonstrates that the neoplastic cells are positive for CD30, with cytoplasmic and faint membrane reactivity. Immunohistochemistry with hematoxylin counterstain, 400×. **D** Axillary lymph node at relapse, 2 years after initial presentation. There is a diffuse infiltrate composed of large cells with vesicular chromatin and distinct nucleolus, admixed with eosinophils. Hematoxylin and eosin, 400×.

lymphoma cells were positive for the B-cell markers CD20 (Fig. 4A), CD79a, and/or PAX5, and showed evidence of EBV infection. All cases were positive for MUM-1/IRF4 and were negative for CD10, supporting a non-germinal center B-cell immunophenotype. BCL6 was positive in two cases. Ki-67 showed a high proliferation rate. All noninvasive cases exhibited an EBV latency pattern type III, positive for EBER (Fig. 4B), LMP-1 (Fig. 4C), and EBNA-2 (Fig. 4D).

The seven noninvasive cases were remarkably similar. B-cell markers highlighted the layering of lymphoma cells between negative zones of granular necrosis. CD30 reactivity was variable (Fig. 4E), ranging from negative in 1 (14%) case (Fig. 4E1), to focal weak (Fig. 4E2) and cytoplasmic (Fig. 4E3) in 5 (72%) cases, to a strong membranous and cytoplasmic pattern (Fig. 4E4) in 1 case. The pattern of CD30 reactivity was uniform in an individual case. Five of six cases were positive for MYC. The lymphoma cells in all cases were positive for CD45, and were negative for T-cell markers, ALK, CD138 (Fig. 4F), EMA, and HHV-8.

Clonality studies using PCR methods were successful in three cases of EBV+ large B-cell lymphoma yielding monoclonal *IGH* rearrangements in all cases. Studies to assess clonality were not performed in the original lesion or the axillary lymph node in the invasive case.

### Comparison with breast implant ALCL

The clinicopathologic and immunophenotypic features of 14 patients with noninvasive breast implant ALCL used for comparison are summarized in Tables 1–3. Patients with EBV+ large B-cell lymphoma more commonly presented with discomfort or pain at the site of implantation, whereas patients with breast implant ALCL distinctly presented with swelling/seroma ($p = 0.0002$). The clinical diagnosis established before surgery was more commonly capsular contracture in patients with EBV+ large B-cell lymphoma ($p = 0.0025$). There were no other significant clinical differences between the cohorts.

The pathologic features of the breast implant ALCL cases have been described previously [6, 24, 25]. Briefly, the median capsular thickness was 1120 µm (range, 543–4347). The luminal side was usually covered by necrosis, sclerosis, or focally by a synovium-like cell layer. Scattered clusters of lymphoma cells were detected floating within the necrosis. The neoplastic cells lined a layer of sclerosis and focally were admixed with inflammatory cells including small lymphocytes, histiocytes, and eosinophils. The lymphoma cells were large and pleomorphic with moderately abundant cytoplasm, and with rare hallmark cells. Karyorrhexis and ghost cells were frequently noted. The mid portion and deeper portions of the capsule were mainly sclerotic with vascular proliferation and scattered inflammatory cells. Small aggregates of lymphocytes as well as birefringent material consistent with silicone were observed in some cases.

We compared the pathologic features of the noninvasive EBV+ large B-cell lymphoma cases with matched noninvasive breast implant ALCL cases (Fig. 5). This comparison showed that noninvasive EBV+ large B-cell lymphoma cases had a thicker capsule ($p = 0.0439$) (Fig. 5A, B), a more prominent layering pattern of the neoplastic cells ($p = 0.005$) (Fig. 5C, D), more frequent calcification or necrosis on the luminal side of the capsule ($p = 0.0112$), (Fig. 5E, F), more frequent presence of foamy histiocytes ($p = 0.0355$), and more frequent presence of lymphoid aggregates in the outer aspects of the capsule ($p < 0.001$) (Fig. 5I, J). Hallmark cells were absent in EBV+ large B-cell lymphoma cases and were common in breast implant ALCL ($p = 0.0039$) (Fig. 5G, H). Cohesive clusters of lymphoma cells were also well delimited from an underlying fibrous layer containing inflammatory cells in cases of breast implant ALCL. There were no other significant differences between the two groups.

**Table 3.** Immunophenotypic and molecular features of patients with noninvasive BI EBV+ LBCL and breast implant ALCL.

| Marker | BI EBV+ LBCL ($n = 7$) | Breast-implant ALCL ($n = 14$) |
|---|---|---|
| CD3 | 0/5 (0%) | **3/14 (21%)** |
| CD4 | 0/2 (0%) | **10/14 (71%)** |
| CD5 | 0/5 (0%) | **2/12 (16%)** |
| CD8 | 0/2 (0%) | **2/14 (14%)** |
| CD10 | 0/7 (0%) | 0/4 (0%) |
| CD15 | 1/2 (50%) | 4/8 (50%) |
| CD20 | **7/7 (100%)** | 0/10 (0%) |
| CD30 | 6/7 (85%) | 14/14 (100%) |
| CD30, intensity | | |
| 1+ | **2 (33%)** | 0 (0%) |
| 2+ | **3 (50%)** | 0 (0%) |
| 3+ | 1 (17%) | **14 (100%)** |
| CD30, extent | | |
| Most lymphoma cells | 3 (50%) | **14 (100%)** |
| Subset lymphoma cells | **3 (50%)** | 0 (0%) |
| CD30, pattern | | |
| Cytoplasmic only | **2 (34%)** | 0 (0%) |
| Cytoplasmic and membrane | 4 (66%) | **14 (100%)** |
| CD43 | 1/2 (50%) | 5/9 (55%) |
| CD45 | **7/7 (100%)** | 3/9 (33%) |
| CD79a | **7/7 (100%)** | 0/4 (0%) |
| CD138 | 0/5 (0%) | NA |
| ALK | 0/7 (0%) | 0/14 (0%) |
| BCL6 | 1/5 (20%) | 0/1 (0%) |
| Epithelial membrane antigen | 0/2 (0%) | **8/10 (80%)** |
| Epstein–Barr virus (EBV) | | |
| EBER[a] | **7/7 (100%)** | 0/7 (0%) |
| EBV LMP-1 | **7/7 (100%)** | NA |
| EBV EBNA-2 | **7/7 (100%)** | NA |
| Latency pattern type III | **7/7 (100%)** | NA |
| Granzyme B | 0/1 (0%) | **5/10 (50%)** |
| HHV-8 | 0/7 (0%) | 0/7 (0%) |
| Ki-67 (%), median | 80% | 90% |
| MUM-1/IRF4 | 7/7 (100%) | 3/3 (100%) |
| MYC | **5/6 (83%)** | NA |
| PAX5 | **6/6 (100%)** | 0/5 (0%) |
| TIA-1 | 0/1 (0%) | **7/9 (77%)** |
| Clonality studies | | |
| *IGH*[b] | 3/3 (100%) | NA |
| *TRB* or *TRG*[b] | NA | 6/6 (100%) |

Bold numbers indicate statistically significant findings.
[a]Epstein–Barr virus-encoded- small RNA, in situ hybridization.
[b]Immunoglobulin heavy chain constant region (*IGH*) and T-cell receptor beta (*TRB*) or gamma (*TRG*).

A comparison of the immunohistochemical features of noninvasive EBV+ large B-cell lymphoma with breast implant ALCL cases showed that the EBV+ large B-cell lymphoma cases, by definition, were positive for B-cell markers whereas breast implant ALCL cases expressed T-cell markers (Fig. 6A, B). CD30 expression was variable in EBV+ large B-cell lymphoma cases, from strong to negative. In contrast, CD30 was strong and uniform in all breast implant ALCL cases. Furthermore, CD30 highlighted layering of lymphoma cells in EBV+ large B-cell lymphoma (Fig. 6C), whereas it showed a distinct demarcation from underlying fibrous tissue in breast implant ALCL (Fig. 6D). All cases of EBV+ large B-cell lymphoma were positive for EBER (Fig. 6E), whereas all cases of breast implant ALCL were negative for EBER (Fig. 6F).

For the comparison of the clinicopathologic and immunophenotypic features of the invasive EBV + large B-cell lymphoma, we lumped our case with two other unique cases reported in the literature, and compared these three cases with 5 cases of invasive breast implant ALCL cases shown in Tables 4 and 5. When compared to invasive EBV + large B-cell lymphoma, cases of invasive breast implant ALCL had an apparent similar median age at diagnosis and a similar time from implantation to lymphoma. Both groups presented with a clinical mass, and histologically there was a variable pattern, including an angiocentric case among the EBV+ large B-cell lymphoma cases. The invasive EBV+ large B-cell lymphoma case we report had invasion of the breast parenchyma, whereas no cases of breast implant ALCL had invasion of breast parenchyma (although we have uncommonly seen breast implant ALCL cases invade breast parenchyma). The background cells, morphology of the lymphoma cells, and pathologic staging were similar in both groups.

## DISCUSSION

We report eight cases of EBV+ large B-cell lymphoma in patients with breast implants, including seven noninvasive cases, and one invasive case that may represent an advanced stage of the spectrum. The noninvasive neoplasms were similar to four noninvasive cases of EBV+ large B-cell lymphoma reported recently by Rodriguez-Pinilla et al. [18] and Mescam et al. [19]. The one invasive case of EBV+ large B-cell lymphoma we report is also similar to two other cases reported in the same series [18, 19].

Over the past two decades, it has become clear that patients with breast implants have an increased risk of developing breast implant ALCL. Rarely, other types of lymphoma have been associated with breast implants including extranodal NK/T-cell lymphoma of nasal type, marginal zone lymphoma, and large B-cell lymphoma [10, 16]. Recently, Rodriguez-Pinilla et al. [18] and Mescam et al. [19] reported four cases of noninvasive EBV+ large B-cell lymphoma that were seemingly clinically indolent, expanding the spectrum of lymphomas in patients with breast implants. The pathogenesis of these neoplasms is uncertain. One opinion is that these cases can be classified as "fibrin-associated large B-cell lymphoma." This type of large B-cell lymphoma is characterized by very small neoplasms that do not form a mass and which are usually detected incidentally. These neoplasms are composed of EBV+ large cells floating in thick fibrinoid clot confined by a fibrous cavity or enmeshed in a thrombus. Fibrin-associated large B-cell lymphoma cases have been detected as a part of the histologic examination of splenic or adrenal pseudocysts, cardiac thrombus, atrial myxomas, or metallic implants [26, 27]. Although EBV+ large B-cell lymphoma cases associated with breast implants do show some similarities with fibrin-associated LBCL, there are also some differences. These differences include the distinctive association of EBV+ large B-cell lymphomas with breast implants with a textured surface, presumably providing a microenvironment that fosters development of lymphoma. As far as is known, the type of surface has not been shown in fibrin-associated large B-cell lymphoma. Another difference is the clinical presentation of these entities. Patients with EBV+ large B-cell lymphoma

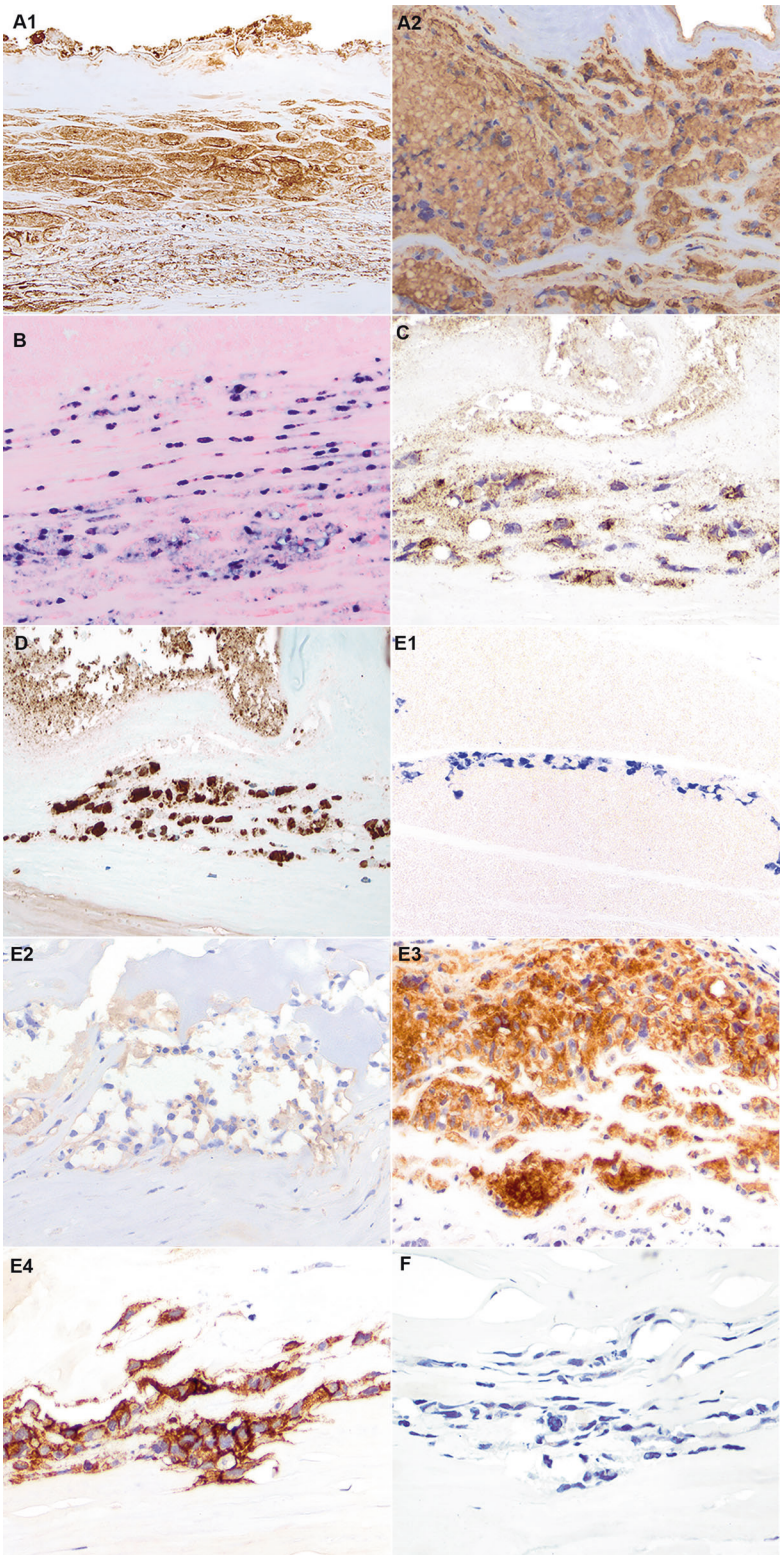


**Fig. 4 Breast-implant EBV+ large B-cell lymphoma: immunohistochemical and in situ hybridization features. A** Immunohistochemistry for CD20 demonstrates cell clusters arranged in layers near the luminal side of the capsule. In this case, there are more viable cells at the bottom, whereas most clusters in mid capsule are extensively necrotic (A1). Note that CD20 reactivity is predominantly cytoplasmic, and barely membranous (A2). Immunohistochemistry for CD20 with hematoxylin counterstain. Left, 100×; right, 400×. **B** In situ hybridization for EBV-encoded RNA (EBER) shows positivity in viable lymphoma cells. Note the layering of lymphoma cells. EBV in situ hybridization, 400×. **C** Immunohistochemistry for EBV latent membrane protein-1 (LMP-1) demonstrates lymphoma cells with cytoplasmic reactivity. Immunohistochemistry for EBV LMP-1 with hematoxylin counterstain, 400×. **D** Immunohistochemistry for Epstein–Barr nuclear antigen 2 (EBNA-2) demonstrates nuclear reactivity of the lymphoma cells. Immunohistochemistry for EBNA-2 with hematoxylin counterstain, 400×. **E** Immunohistochemistry for CD30 demonstrates the variability of expression in different cases of breast implant EBV+ large B-cell lymphoma. Negative (E1), faint, cytoplasmic (E2); cytoplasmic (E3); and strong membranous and cytoplasmic (E4). Immunohistochemistry for CD30 with hematoxylin counterstain, 400×. **F** Immunohistochemistry for CD138 demonstrates that the lymphoma cells are negative. Immunohistochemistry for CD138 with hematoxylin counterstain, 400×.

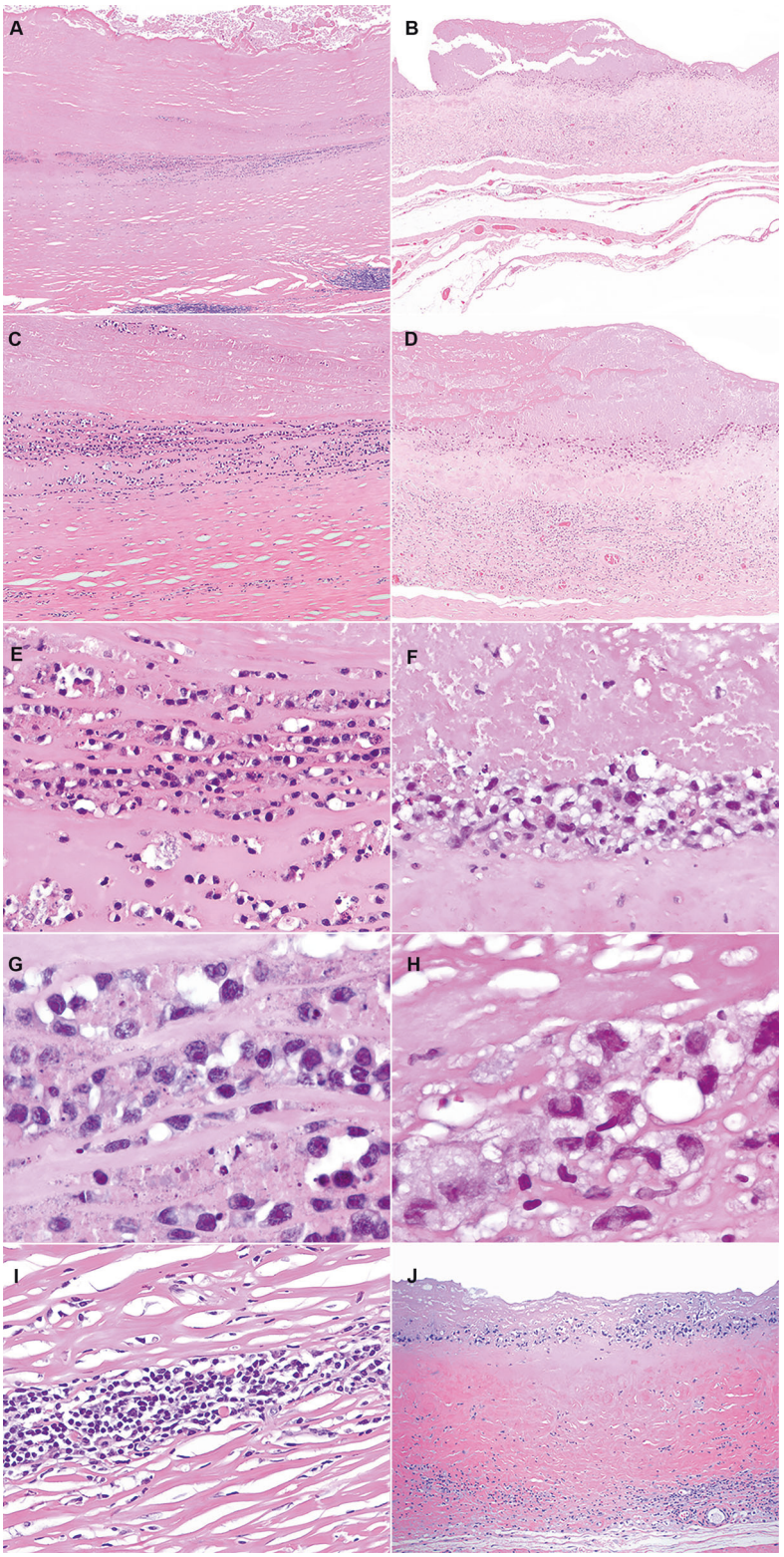


**Fig. 5 Comparison of histological features of breast implant EBV+ large B-cell lymphoma and breast implant anaplastic large cell lymphoma (breast implant ALCL).** The capsular composition shows significantly more layering of lymphoma cells and sclerosis in breast implant EBV+ large B-cell lymphoma (**A, C**) than in breast implant ALCL (**B, D**) ($p < 0.005$), while the presence of necrosis is similar ($p > 0.99$). Hematoxylin and eosin, 40× (**A, B**) and 100× (**C, D**). Lymphoma cell aggregates with a layering pattern are noted in breast implant EBV+ large B-cell lymphoma (**E**), while lymphoma cells cluster along the fibrous capsule in breast implant ALCL (**F**). Hematoxylin and eosin, 400×. Lymphoma cells are large, and round to oval with vesicular chromatin admixed with karyorrhexis in breast implant EBV+ large B-cell lymphoma (**G**), whereas the cells are more variable and pleomorphic, including occasional "hallmark" cells in breast implant ALCL (**H**). Hematoxylin and eosin, 1000×. Outer capsule lymphoid aggregates, commonly associated with numerous plasma cells in the outer aspect of the capsule, away from lymphoma cells were noted in cases of breast implant EBV+ large B-cell lymphoma. (**I**) Sclerosis admixed with small lymphocytes, histiocytes, and plasma cells were noted in the outer capsule of cases of breast implant ALCL (**J**). ($p = 0.25$ for lymphoid aggregates). Hematoxylin and eosin, 400×.

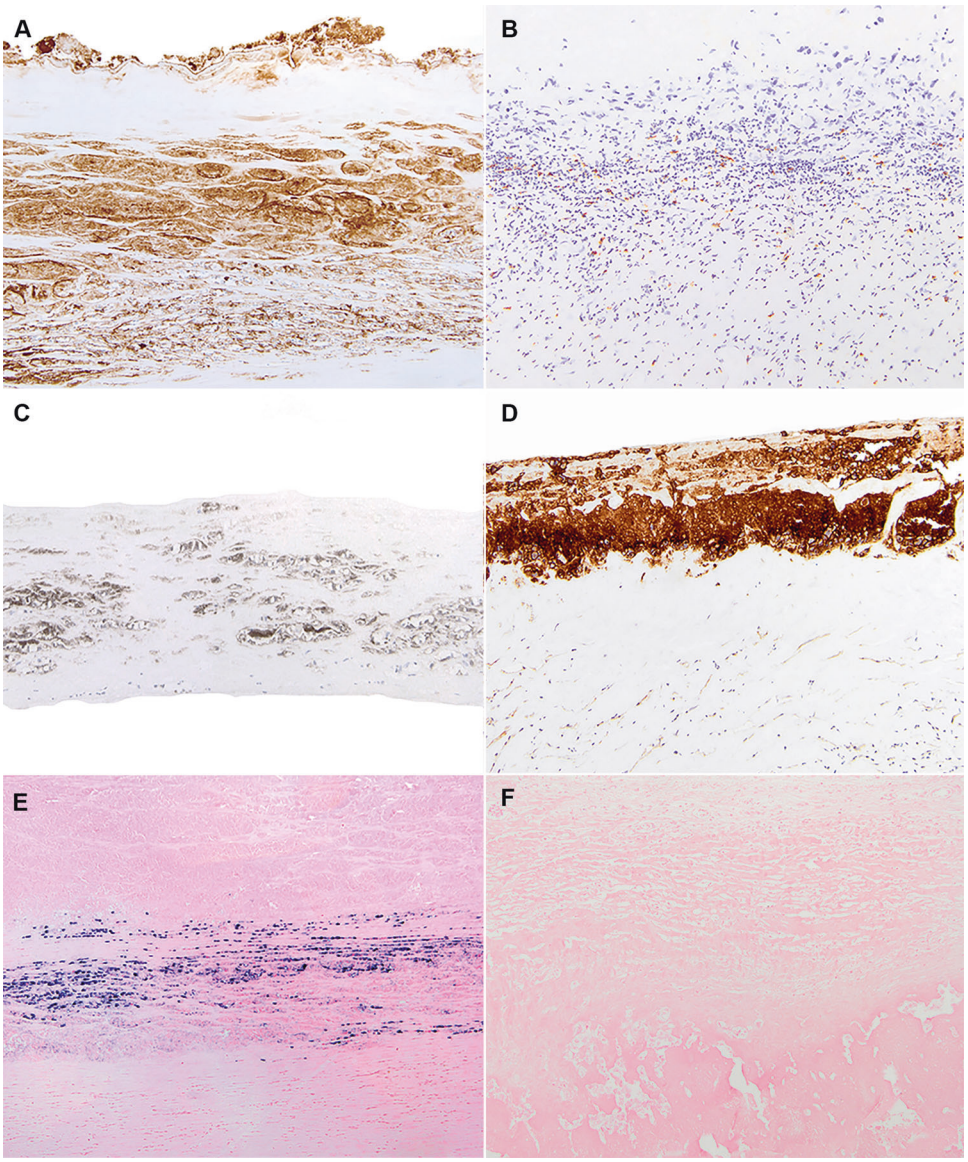


**Fig. 6 Comparison of the immunophenotypic features between noninvasive breast implant EBV+ LBCL and breast implant ALCL, pathologic stage T2. A, B** Immunohistochemistry with anti-CD20. **A** Numerous clusters of lymphoma cells display a layering pattern in a cases of breast implant EBV+ large B-cell lymphoma. **B** The neoplastic cells are negative for CD20, with rare small lymphocytes highlighted in this case of breast implant ALCL. 100×. **C, D** Immunohistochemistry with anti-CD30. **C** Layering of lymphoma cells in cases of breast implant EBV+ large B-cell lymphoma. **D** Apparent cohesiveness of cells above the collagenous capsule in a case of breast implant ALCL; the fibrinoid and necrotic cells at the luminal side appear as unevenly positive. Immunohistochemistry for CD30 with hematoxylin counterstain. 100×. **E, F** In situ hybridization for EBV-encoded RNA (EBER). **E** Layers of cells are highlighted with EBER in a case of breast implant EBV+ large B-cell lymphoma. **F** Neoplastic cells are negative for EBER in cases of breast implant ALCL. EBV-encoded RNA in situ hybridization, 100×.

associated with breast implants usually present with local symptoms, unlike the typical incidental discovery of fibrin-associated large B-cell lymphoma in affected patients. Last, the latency interval between breast implantation and development of EBV+ large B-cell lymphoma was consistently several years. By contrast, a latency interval is not established for fibrin-associated LBCL, although large intervals have been observed for the subset of patients with vascular prostheses. With longer clinical follow up, other differences may emerge between EBV+ large B-cell lymphoma associated with breast implants versus fibrin-associated large B-cell lymphoma.

An alternative hypothesis is that the etiology of EBV+ large B-cell lymphoma is related uniquely to the presence of breast implants, analogous to the etiology of breast implant ALCL itself. In support of this suggestion, EBV+ large B-cell lymphoma occurs only in patients with textured breast implants, analogous to breast implant ALCL. In our opinion, both textured and smooth breast implants would likely be involved if EBV+ large B-cell lymphoma arose via mechanisms analogous to fibrin-associated large B-cell lymphoma. It is also true that patients with EBV+ large B-cell lymphoma presented clinically with findings very similar to breast implant ALCL, prompting suspicion of the diagnosis before the surgical procedure, and histologic examination revealed EBV+ large B-cell lymphoma. As observed in patients with breast implant ALCL, there was a long latency interval between implantation and development of EBV + large B-cell lymphoma. In addition, the morphologic findings of EBV+ large B-cell lymphoma overlap greatly with breast

**Table 4.** Clinicopathologic features, therapy, and outcomes of invasive EBV+ large B-cell lymphoma in patients with breast implants.

| Features | Current case | Rodriguez-Pinilla et al. | Mescam et al. | BI ALCL invasive cases ($n = 5$) |
|---|---|---|---|---|
| Clinical features | | | | |
| Age (years) | 48 | 63 | 61 | Median: 57 (range: 41–72) |
| Reason for implant | NA | Reconstruction | Reconstruction | Cosmetic (4), reconstruction post breast cancer (1) |
| Filling of implant | Silicone | NA | NA | Saline (2), silicone (2) |
| Surface of implant | NA | NA | Textured | Textured (2) |
| Make of implant | NA | NA | Allergan | Allergan (1) |
| Years from implantation to lymphoma | 21 | 20 | 13 | Median: 12 (range: 5–25) |
| Clinical presentation | Nodularity | Local mass | Asymptomatic | Mass (2), capsule thickening (1), effusion (1), breast pain and capsule contraction (1) |
| Clinical diagnosis | Tumor mass | Mass | Incidental | Mass (5) |
| Pathologic features | | | | |
| Pattern | Sclerosis | Angiocentric | Multinodular | Multinodular (2), diffuse (2), and sclerotic and multinodular (1) |
| Background cells | Small lymphocytes, histiocytes, eosinophils | Plasma cells, lymphoid follicles with germinal centers | Plasma cells, lymphoid follicles | Histiocytes (5), small lymphocytes (4), plasma cells (4), and eosinophils (4) |
| Breast parenchyma invasion | Yes | NA | | No (5) |
| Lymphoma cell features | Large, lobated | Large, Reed–Sternberg like cells | Plasmablastic | Large, lobated (5) |
| Staging | | | | |
| Clinical stage | IE | IE | IE | II (3), IE (1), IIB (1) |
| Pathologic stage | pT4 | pT4 | pT4 | pT4 (5) |
| Therapy | | | | |
| Complete capsulectomy | Yes | Yes | Yes | Yes (5) |
| Chemotherapy regimen | CHOP 4 cy; BEACOPP 2 cy; RT; ICE; ASCT | NA | None | CHOP 6 cy (1); CHOP 3 cy plus ICE (1); R-EPOCH plus Brentuximab (1) |
| Radiation therapy | Yes | NA | None | Yes (2) |
| Follow up and outcomes | | | | |
| Time from initial presentation (mo) | 71 | NA | 21 | median: 76 (range: 45–143) |
| Time after diagnosis (mo) | 8 | 2 | 21 | median: 50 (range: 40–119) |
| Outcome | CR | NA | CR | CR (4) and PR (1) |

*ASCT* autologous stem cell transplant, *BEACOPP* bleomycin, etoposide, Adriamycin, cyclophosphamide, vincristine (Oncovin), procarbazine, prednisone, *CHOP* cyclophosphamide, Adriamycin, vincristine, prednisone, *CR* complete remission, *Cy* cycles of chemotherapy, *ICE* ifosfamide, carboplatin, etoposide, *pT4* pathologic stage 4, *PR* partial remission.

implant ALCL. In our comparison of EBV+ large B-cell lymphoma with breast implant ALCL, there were few significant morphologic differences. Last, patients with noninvasive EBV+ large B-cell lymphoma had an excellent outcome after removal of implant and complete capsulectomy, similar to patients with breast implant ALCL. Therefore, we suggest that the evidence in aggregate suggests that the pathogenesis of EBV+ large B-cell lymphoma is uniquely related to textured breast implants and differs, at least in part, from cases of fibrin-associated large B-cell lymphoma. This conclusion is in line with the opinion of Rodriguez-Pinilla et al. [18] who suggested the term breast-implant-associated EBV+ large B-cell lymphoma. The pathogenic mechanisms are not yet understood, but localized immunosuppression with high IL-10 levels as well as hypoxia have been postulated [28, 29].

In conclusion, this report of eight cases of EBV+ large B-cell lymphoma in association with breast implants expands the spectrum of lymphomas that are associated with breast implants. We believe that this case series as well as a smaller number of cases reported in the literature show that the spectrum of EBV+ large B-cell lymphoma closely matches the clinical and pathologic features of breast implant ALCL. In addition, these neoplasms are associated with textured implants, and patients have an excellent outcome after implant removal and complete capsulectomy, which is the standard of care for patients with breast implant ALCL [6, 9]. We therefore suggest that textured breast implants as well as EBV infection are involved, and likely essential, in the pathogenesis of cases of EBV+ large B-cell lymphoma associated with breast implants.

## DATA AVAILABILITY

Data are confidential and not available to review by external sources.

**Table 5.** Immunophenotypic, genetic, and molecular features of invasive EBV+ large B-cell lymphomas in patients with breast implants.

| | Current case | Rodriguez-Pinilla et al. | Mescam et al. | BI ALCL invasive cases ($n = 5$) |
|---|---|---|---|---|
| B-cell markers | | | | |
| CD19 | Neg | NA | NA | NA |
| CD20 | Neg | Pos | NA | Neg (5/5) |
| CD79a | Focal Weak | Pos, focal | Pos, focal | Neg (2/2) |
| PAX5 | Pos | Neg | NA | Neg (2/2) |
| T-cell markers | | | | |
| CD3 | Neg | Pos | NA | Neg (4/5) |
| CD4 | Weak, focal | Neg | Weak, focal | Pos (5/5) |
| CD5 | Neg | NA | NA | Neg (3/5) |
| CD7 | Neg | NA | NA | Neg (3/3) |
| CD8 | Neg | Neg | NA | Neg (4/5) |
| CD43 | Neg | NA | NA | Pos (4/4) |
| Plasma cell markers | | | | |
| CD138 | Neg | NA | Neg | NA |
| Kappa | NA | Polytypic | Pos | NA |
| Lambda | NA | Polytypic | Neg | NA |
| Cytotoxic markers | | | | |
| Granzyme B | Neg | Pos | NA | Pos (3/5) |
| Perforin | Neg | Pos | NA | Pos (1/2) |
| TIA-1 | NA | Pos | NA | Pos (3/5) |
| Activation markers | | | | |
| CD25 | Neg | NA | NA | Pos (4/4) |
| CD30 | Membrane | Pos | Pos focal | Pos (5/5) |
| Cell of Origin | Non-GC | NA | Non-GC | Non-GC |
| CD10 | Neg | NA | Pos focal | Neg (1/1) |
| BCL6 | Neg | NA | Pos focal | Neg (2/3) |
| MUM-1 | Pos | Pos | Pos | NA |
| Viral markers | | | | |
| Epstein–Barr virus (EBV) status | | | | |
| EBER | Pos | Pos | Pos | Neg (4/4) |
| LMP-1 | Pos | Pos, few | Neg | NA |
| EBNA-2 | Neg | Pos | Neg | NA |
| latency type | II | III | I | NA |
| HHV-8 | Neg | Neg | Neg | NA |
| Other markers | | | | |
| CD15 | Pos | NA | NA | Pos (1/2) |
| CD34 | Neg | NA | NA | Neg (3/3) |
| CD45 | Neg | NA | Pos | Pos (5/5) |
| CD45-RO | Neg/focal | NA | NA | NA |
| CD56 | NA | Neg | Neg | Neg (5/5) |
| ALK-1 | Neg | NA | NA | Neg (5/5) |
| Epithelial membrane antigen | Neg | NA | NA | Pos (2/3) |
| Myc | NA | Neg | 70% | NA |
| p53 | NA | Neg | NA | NA |
| p-STAT3 | NA | NA | Pos | NA |
| T-cell receptor | | | | |
| βF1 | NA | Neg | NA | Neg (3/5) |
| γ | NA | Neg | NA | Neg (5/5) |
| Clonality | | | | |
| *IGH* | NA | NA | Monoclonal | Neg (1/1) |
| *TRB* | NA | NA | NA | Neg (1/1) |

**Table 5** continued

| | Current case | Rodriguez-Pinilla et al. | Mescam et al. | BI ALCL invasive cases ($n = 5$) |
|---|---|---|---|---|
| *TRG* | NA | NA | NA | Neg (1/1) |
| T-cell receptor, NOS | NA | NA | Minor, 10% | NA |
| FISH | | | | |
| *IGH-MYC* | NA | NA | Pos | NA |
| *BCL2* rearrangement | NA | NA | Neg | NA |
| *BCL6* rearrangement | NA | NA | Neg | NA |
| Next-generation sequencing | | | | |
| Mutations | NA | NA | *STAT3, SOCS1, FOXO1, CCND2* | NA |

## REFERENCES

1. Talwalkar SS, Miranda RN, Valbuena JR, Routbort MK, Martin AW, Medeiros LJ. Lymphomas involving the breast: a study of 106 cases comparing localized and disseminated neoplasms. Am J Surg Pathol. 2008;32:1299–309.
2. Keech JA, Creech BJ. Anaplastic T-cell lymphoma in proximity to a saline-filled breast implant. Plast Reconstr Surg. 1997;100:554–5.
3. Lyapichev KA, Medeiros LJ, Clemens MW, Ferrufino-Schmidt MC, Marques-Piubelli ML, Chai SM, et al. Reconsideration of the first recognition of breast implant-associated anaplastic large cell lymphoma: a critical review of the literature. Ann Diagn Pathol. 2020;45:151474.
4. Feldman AL, Harris NL, Stein H, Campo E, Kinney MC, Jaffe ES, et al. Breast implant-associated anaplastic large cell lymphoma. In: Swerdlow SH, Campo E, Harris NL, Jaffe ES, Pileri SA, Stein H, Thiele J, editors. WHO classification of tumours of haematopoietic and lymphoid tissues (Revised 4th edition). Lyon: IARC; 2017. p. 421–2.
5. Miranda RN, Feldman AL, Soares FA. Breast implant-associated anaplastic large cell lymphoma. In: Allison KH, et al., editors. World Health Organization breast tumours. Lyon: IARC; 2019. p. 245–8.
6. Clemens MW, Medeiros LJ, Butler CE, Hunt KK, Fanale MA, Horwitz S, et al. Complete surgical excision is essential for the management of patients with breast implant-associated anaplastic large-cell lymphoma. J Clin Oncol. 2016;34:160–8.
7. Miranda RN, Aladily TN, Prince HM, Kanagal-Shamanna R, de Jong D, Fayad LE, et al. Breast implant-associated anaplastic large-cell lymphoma: long-term follow-up of 60 patients. J Clin Oncol. 2014;32:114–20.
8. Laurent C, Delas A, Gaulard P, Haioun C, Moreau A, Xerri L, et al. Breast implant-associated anaplastic large cell lymphoma: two distinct clinicopathological variants with different outcomes. Ann Oncol. 2016;27:306–14.
9. Clemens MW, Horwitz SM. NCCN consensus guidelines for the diagnosis and management of breast implant-associated anaplastic large cell lymphoma. Aesthet Surg J. 2017;37:285–9.
10. Aladily TN, Nathwani BN, Miranda RN, Kansal R, Yin CC, Protzel R, et al. Extranodal NK/T-cell lymphoma, nasal type, arising in association with saline breast implant: expanding the spectrum of breast implant-associated lymphomas. Am J Surg Pathol. 2012;36:1729–34.
11. Cook PD, Osborne BM, Connor RL, Strauss JF. Follicular lymphoma adjacent to foreign body granulomatous inflammation and fibrosis surrounding silicone breast prosthesis. Am J Surg Pathol. 1995;19:712–7.
12. Kraemer DM, Tony HP, Gattenlohner S, Muller JG. Lymphoplasmacytic lymphoma in a patient with leaking silicone implant. Haematologica. 2004;89:ELT01.
13. Moling O, Piccin A, Tauber M, Marinello P, Canova M, Casini M, et al. Intravascular large B-cell lymphoma associated with silicone breast implant, HLA-DRB1*11:01, and HLA-DQB1*03:01 manifesting as macrophage activation syndrome and with severe neurological symptoms: a case report. J Med Case Rep. 2016;10:254.
14. Nichter LS, Mueller MA, Burns RG, Stallman JM. First report of nodal marginal zone B-cell lymphoma associated with breast implants. Plast Reconstr Surg. 2012;129:576e–8e.
15. Smith BK, Gray SS. Large B-cell lymphoma occurring in a breast implant capsule. Plast Reconstr Surg. 2014;134:670e–1e.
16. Evans MG, Miranda RN, Young PA, Pai L, Wang H-Y, Konoplev SN, et al. B-cell lymphomas associated with breast implants: report of three cases and review of the literature. Ann Diagn Pathol. 2020;46:151512.
17. Geethakumari PR, Markantonis J, Shah JL, Alsuwaidan A, Shahab I, Chen W, et al. Breast implant-associated plasmablastic lymphoma: a case report and discussion of the literature. Clin Lymphoma Myeloma Leuk. 2019;19:e568–72.
18. Rodríguez-Pinilla SM, García FJ, Balagué O, Rodríguez-Justo M, Piris M. Breast implant-associated Epstein–Barr virus-positive large B-cell lymphomas: a report of three cases. Haematologica. 2020;105:e412–4.
19. Mescam L, Camus V, Schiano JM, Adelaide J, Picquenot JM, Guille A, et al. EBV+ diffuse large B-cell lymphoma associated with chronic inflammation expands the spectrum of breast implant-related lymphomas. Blood. 2020;135:2004–9.
20. Vega F, Medeiros LJ, Jones D, Abruzzo LV, Lai R, Manning JT, et al. A novel four-color PCR assay to assess T-cell receptor gamma gene rearrangements in lymphoproliferative lesions. Am J Clin Pathol. 2001;116:17–24.
21. Tevis SE, Hunt KK, Miranda RN, Lange C, Pinnix CC, Iyer S, et al. Breast implant-associated anaplastic large cell lymphoma: a prospective series of 52 patients. Ann Surg. 2020. https://doi.org/10.1097/sla.0000000000004035.
22. Miranda RN, Lin L, Talwalkar SS, Manning JT, Medeiros LJ. Anaplastic large cell lymphoma involving the breast: a clinicopathologic study of 6 cases and review of the literature. Arch Pathol Lab Med. 2009;133:1383–90.
23. Khoo C, McTigue C, Hunter-Smith DJ, Walker P. EBV positive fibrin/chronic inflammation associated diffuse large B-cell lymphoma: an incidental finding associated with a breast implant. Pathology. 2020. https://doi.org/10.1016/j.pathol.2020.09.022.
24. Aladily TN, Medeiros LJ, Amin MB, Haideri N, Ye D, Azevedo SJ, et al. Anaplastic large cell lymphoma associated with breast implants: a report of 13 cases. Am J Surg Pathol. 2012;36:1000–8.
25. Quesada AE, Medeiros LJ, Clemens MW, Ferrufino-Schmidt MC, Pina-Oviedo S, Miranda RN. Breast implant-associated anaplastic large cell lymphoma: a review. Mod Pathol. 2019;32:166–88.
26. Boroumand L, Ly TL, Sonstein J, Medeiros LJ. Microscopic diffuse large B-cell lymphoma (DLBCL) occurring in pseudocysts: do these tumors belong to the category of DLBCL associated with chronic inflammation? Am J Surg Pathol. 2012;36:1074–80.
27. Boyer DF, McKelvie PA, de Leval L, Edlefsen KL, Ko Y-H, Aberman ZA, et al. Fibrin-associated EBV-positive large B-cell lymphoma: An indolent neoplasm with features distinct from diffuse large B-cell lymphoma associated with chronic inflammation. Am J Surg Pathol. 2017;41:299–312.
28. Di Napoli A, Greco D, Scafetta G, Ascenzi F, Gulino A, Aurisicchio L, et al. IL-10, IL-13, Eotaxin and IL-10/IL-6 ratio distinguish breast implant-associated anaplastic large-cell lymphoma from all types of benign late seromas. Cancer Immunol Immunother. 2021;70:1379–92.
29. Oishi N, Hundal T, Phillips JL, Dasari S, Hu G, Viswanatha DS, et al. Molecular profiling reveals a hypoxia signature in breast implant-associated anaplastic large cell lymphoma. Haematologica. 2020. https://doi.org/10.3324/haematol.2019.245860.

## AUTHOR CONTRIBUTIONS

All authors were involved in the design, writing, and final approval of the manuscript.

## FUNDING

Department of Hematopathology at The University of Texas MD Anderson Cancer Center.

## COMPETING INTERESTS

The authors declare no competing interests.

## ETHICS APPROVAL AND CONSENT TO PARTICIPATE

This study was been approved by the Institutional Review Board. Patients consented to participate in research study.

## ADDITIONAL INFORMATION

**Correspondence** and requests for materials should be addressed to R.N.M.

**Reprints and permission information** is available at http://www.nature.com/reprints

**Publisher's note** Springer Nature remains neutral with regard to jurisdictional claims in published maps and institutional affiliations.